MMA Memo 210

Radiometric Phase Correction

C.L. Carilli

National Radio Astronomy Observatory

Socorro, NM, 87801

ccarilli@nrao.edu

O. Lay

University of California at Berkeley

Radio Astronomy Laboratory

Berkeley, CA, 94720

olay@astron.berkeley.edu

E.C. Sutton

University of Illinois

Department of Astronomy

Urbana, IL, 61801

sutton@astro.uiuc.edu

January 15, 1998

Abstract

We analyze the technique of using radiometers to measure the precipitable water vapor (PWV) content of the atmosphere in order to correct interferometric data for phase noise due PWV fluctuations in the troposphere. We present an idealized model of phase fluctuations due to PWV variations in the troposphere based on the Taylor hypothesis, and we summarize the radiometry equations. We then consider various options for radiometric phase corrections, including: (i) the very demanding technique of making an absolute measurement of PWV at each antenna assuming an accurate (absolutely calibrated) measurement of brightness temperature, T_B, and using a theoretical model for the troposphere and measured physical parameters for the troposphere (temperature, pressure, etc...), and (ii) the less demanding technique of using a strong celestial calibration source to derive an empirical relationship between brightness temperature fluctuations and atmospheric phase fluctuations.

Radiometric phase correction requires systems that are sensitive ($19 \leq T_{rms} \leq 920$ mK), and stable over long timescales ($200 \leq \delta\mathrm{Gain} \leq 15000$). Absolute radiometric phase correction at each antenna also requires knowledge of the tropospheric parameters, such as T_{atm}, P_{atm}, and h_{turb}, to a few percent or less. And even if such accurate measurements are available, fundamental uncertainties in the atmospheric models relating T_B and PWV may require empirical calibration of the T_B^{rms} - w_{rms} relationship at regular intervals.

The empirical approach increases the coherence time of the array, but a number questions remain to be answered, including: (i) over what time scale and distance will this technique allow for radiometric phase corrections when switching between the source and the calibrator?, and (ii) how often will calibration of the T_B^{rms} - θ_{rms} relationship be required, ie. how stable are the mean parameters of the atmosphere?

1. Introduction

The radiometry equation (Dicke et al. 1946) relates the observed brightness temperature of the sky, T_B, to the atmospheric temperature, T_{atm}, and the total optical depth through the atmosphere, τ_{tot}, as:

$$T_B = T_{atm} \times (1 - e^{-\tau_{tot}}). \qquad (1)$$

The opacity is due to the pressure broadened wings of various mm, sub-mm, and IR lines of water vapor, O_2, and other trace gases (CO,N_2O,...). The contribution from O_2 and other trace gases is thought to be stable over time. The water vapor contribution can be time variable. This has led to the hypothesis that by measuring fluctuations in T_B with a radiometer, one can derive the fluctuations in the column density of water vapor of the troposphere (Barrett and Chung 1962, Staelin 1966, Westwater and Guiraud 1980, Rosenkranz 1989). This column density is usually quantified in terms of the effective depth of water vapor converted to the liquid phase: w = milli-meters of precipitable water vapor (PWV).

Water vapor affects the index of refraction of the troposphere, hence variations in PWV lead to variations in the effective electrical path length, corresponding to variations in the phase of a electromagnetic wave propagating through the troposphere (Tatarskii 1978). Such variations are seen as 'phase noise' by radio interferometers. Since the effect increases linearly with frequency (except in the vicinity of the strong water lines), such variations are most prominent for mm and sub-mm interferometers, and phase variations caused by tropospheric PWV fluctuations can be the limiting factor for the coherence time and spatial resolution of mm interferometers (Hinder and Ryle 1971).

Many groups have proposed to reduce tropospheric phase variations by measuring fluctuations in PWV using radiometers (Resch, Hogg, and Napier 1984, Bagri 1994, Woody and Marvel 1998). The correlation between T_B and interferometer phase has been demonstrated by a number of groups (Bagri 1994, Resch, Hogg, and Napier 1984). However, the conversion of these values to antenna-based electrical phase, and the subsequent application of these phases to interferometric data, has met with mixed success (Welch 1994, Bremer, Guilloteau, and Lucas, R. 1997).

In this memorandum we investigate the technique of using radiometers to reduce tropospheric phase fluctuations, both in the context of the MMA site at Chajnantor, and at the VLA site. We present an idealized model of phase fluctuations due to PWV variations in the troposphere based on the Taylor hypothesis. We then summarize the radiometry equations, and we consider various options for radiometric phase corrections. We begin by considering the very stringent requirement of making an absolute measurement of PWV at each antenna assuming an accurate (absolutely calibrated) measurement of brightness temperature, and using a theoretical model for the troposphere and measured physical parameters for the troposphere (temperature, pressure, etc...). We then consider the less demanding technique of using a strong celestial calibration source to derive an empirical relationship between brightness temperature fluctuations and atmospheric phase fluctuations at regular intervals.

2. Tropospheric phase fluctuations: the root phase structure function

The standard model for tropospheric phase fluctuations involves variations in the water vapor column density in a turbulent layer in the troposphere with a mean height, h_{turb}, and a vertical extent, W, which moves at some velocity, V_A. This model includes the 'Taylor hypothesis', or 'frozen screen approximation', which states that: 'if the turbulent intensity is low and the turbulence is approximately stationary and homogeneous, then the turbulent field is unchanged over the atmospheric boundary layer time scales of interest and advected with the mean wind' (Taylor 1938, Garratt 1992). Under this assumption one can relate temporal and spatial phase fluctuations with a simple Eulerian transformation using V_A. In the following sections we adopt a value of $V_A = 10$ m s^{-1}.

Tropospheric phase fluctuations are usually characterized by a root phase structure function, Φ_{rms}(b), equal to the root mean square phase variations on baselines of length b, when calculated over a sufficiently long time (time >> baseline crossing time = $\frac{b}{V_A}$), or for an ensemble of measurements at a given time on many baselines of length b. Kolmogorov turbulence theory (Coulman 1990) predicts a function of the form:

$$\Phi_{rms}(b) = \frac{K}{\lambda}\, b^n \quad degrees \qquad (2)$$

where b is in km, and λ is in mm. In this report we adopt a typical value of K = 100 for the MMA site in Chajnantor, and K = 300 for the VLA site (Carilli, Holdaway, and Sowinski 1996).

Kolmogorov turbulence theory predicts n = $\frac{1}{3}$ for baselines longer than W, and n = $\frac{5}{6}$ for baselines shorter than W (Coulman 1990). The change in power-law index at b = W is due to the finite vertical extent of the turbulent layer. For baselines shorter than the typical turbulent layer extent the full 3-dimensionality of the turbulence is involved (thick-screen), while for longer baselines a 2-dimensional approximation applies (thin-screen). Turbulence theory also predicts an 'outer-scale', L_o, beyond which the rms phase should no increase with baseline length (ie. n = 0). This scale corresponds to the largest coherent structures, or maximum correlation length, for water vapor fluctuations in the troposphere, presumably set by external boundary conditions.

Recent observations with the VLA by Carilli and Holdaway (1997) support Kolmogorov theory for tropospheric phase fluctuations. Their result is reproduced in Figure 1, which shows the root phase structure function made using the BnA configuration of the VLA. This configuration has good baseline coverage ranging from 200m to 20 km, hence sampling all three hypothesized ranges in the structure function. Observations were made during the night of Jan. 27, 1997 using the VLA calibration source 0748+240. The total observing time was 90 min, corresponding to a tropospheric travel distance of 54 km, assuming V_A = 10 m s^{-1}. The open circles show the nominal tropospheric root phase structure function over the full 90 min time range. The solid squares are the rms phases after subtracting (in quadrature) a constant electronic noise term of 10°, as derived from the data by requiring the best power-law on short baselines. The 10° noise term is consistent with previous measurements at the VLA indicating electronic phase noise increasing with frequency as 0.5° per GHz (Carilli and Holdaway 1996).

The three regimes of the structure function as predicted by Kolmogorov theory are verified in Figure 1. On short baselines (b $\leq$ 1.2 km) the measured power-law index is 0.85$\pm$0.03 and the predicted value is 0.83. On intermediate baselines (1.2 $\leq$ b $\leq$ 6 km) the measured index is 0.41$\pm$ 0.03 and the predicted value is 0.33. On long baselines (b $\geq$ 6 km) the measured index is 0.1$\pm$0.2 and the predicted value is zero. The implication is that the vertical extent of the turbulent layer is: W $\approx$ 1 km, and that the outer scale of the turbulence is: L_o $\approx$ 6 km. The increase in the scatter of the rms phases for baselines longer than 6 km may be due to an anisotropic outer scale (see Carilli and Holdaway 1997).

3. Atmospheric Opacity Models and Basic Assumptions

A rigorous treatment of the radiometry equation (1) involves integration of the radiative transfer equations through the atmosphere using the vertical profiles of temperature and density, and using models for the spectral line shapes. There are number of codes which generate synthetic atmospheric optical depth and T_B spectra using extensive lists of spectral lines from atmospheric constituents under various conditions (Liebe 1989, Sutton and Hueckstaedt 1997). One well known problem with these models is that they substantially under-predict T_B for a given amount of PWV, in particular for measurements made away from the water lines. The likely cause of this discrepancy is incorrect line shapes far into the wings of the lines (Sutton and Hueckstaedt 1997). Hence, many codes also include empirically determined 'water vapor continuum fudge-factors' to mitigate this discrepancy. If this discrepancy is due to incorrect line shapes, then these fudge-factors may be functions of both atmospheric pressure and temperature, and hence are likely to be time variable (section 5).

For the purposes of the calculations presented herein we have used the atmospheric model of Liebe (1989), as maintained by Holdaway and Pardo (1997). This model includes a local line base of 44 O_2 lines plus 30 H_2O lines plus lines from trace gases in the range from 20 GHz to 1000 GHz, and an empirical (power-law) correction for the 'water vapor continuum'. The code employs the U.S. Standard Model Atmosphere, for which the ground temperature and pressure at the MMA site are: 270 K and 560 mb, respectively. The corresponding values for the VLA site are: 287 K and 790 mb. A linear gradient of temperature with elevation of -6 K km^{-1} is assumed.

For the MMA the site elevation is 5000 m (Chajnantor), and the typical optical depth at 230 GHz is 0.06, implying a mean w = 1 mm (Holdaway and Pardo 1997). For the VLA the site elevation is 2150 m and the typical opacity at 43 GHz is 0.06, implying a mean w = 5 mm. Plots of the atmospheric T_B and transmission for the MMA and VLA sites under these assumptions are shown in Figures 2 and 3, for frequencies ranging from 0 to 1000 GHz. Figures 4 and 5 are blow-ups of the optical depth from 0 to 250 GHz, with the different components (PWV and other gases) shown explicitly.

4. Sensitivity Requirements for Radiometric Phase Corrections

We assume that the atmospheric opacity can be divided into three parts:

$$\tau_{tot} \ = \ A_\nu \times w_o \ + \ B_\nu \ + \ A_\nu \times w_{rms}, \qquad (3)$$

where: (i) A_ν is the optical depth per mm of PWV (Figures 4 and 5) as a function of frequency, (ii) w_o is the temporally stable (mean) value for PWV of the troposphere, (iii) B_ν is the total optical depth due to all other gases besides water as a function of frequency (also assumed to be temporally stable), and (iv) w_{rms} is the time variable component of the PWV of the troposphere. It is this time variable component which causes the tropospheric phase 'noise' for an interferometer. In effect, we assume a constant mean optical depth: $\tau_o \equiv A_\nu \times w_o \ + \ B_\nu$, with a fluctuating term due to changes in PWV: $\tau_{rms} \equiv A_\nu \times w_{rms}$, and that $\tau_o >> \tau_{rms}$.

Inserting (3) into equation (1), and making the reasonable assumption that $A_\nu \times w_{rms} << 1$, leads to:

$$T_B \ = \ T_{atm} \times [1 - e^{-\tau_o}] \ \ + \ \ T_{atm} \times e^{-\tau_o} \times [A_\nu \times w_{rms} \ + \ \frac{(A_\nu \times w_{rms})^2}{2} \ + \ ...] \qquad (4)$$

The first term on the righthand side of equation (4) represents the mean, non-varying T_B of the troposphere. The second term represents the fluctuating component due to variations in PWV, which we define as:

$$T_B^{rms} \ \equiv \ T_{atm} \times e^{-\tau_o} \times [A_\nu \times w_{rms} \ + \ \frac{(A_\nu \times w_{rms})^2}{2} \ + \ ...] \qquad (5)$$

At first glance, it would appear that equation (5) applies to fluctuations in a turbulent layer at the top of the troposphere, since the fluctuating component is fully attenuated (ie. multiplied by $e^{-\tau_o}$). However, for a turbulent layer at lower altitudes there is the additional term of attenuation of the atmosphere above the turbulent layer by the turbulence. It can be shown that the terms exactly cancel for an isobaric, isothermal atmosphere, in which case equation 5 is *independent* of the height of the turbulence.

We can then use the relationships between w and electrical pathlength to derive the phase fluctuations due to the troposphere. The electrical pathlength, L, is given by: L$\approx$6.5$\times$w, across most of the mm to sub-mm spectrum, except in the vicinity of the strong water lines where dispersive effects become significant (Hogg, Guiraud, and Decker 1981). The extra phase, ϕ, introduced to a propagating electromagnetic wave is then:

$$\phi \;=\; 2\pi \times \frac{L}{\lambda} \;=\; 13\pi \times \frac{w}{\lambda} \;\; rad. \qquad (6)$$

The absolute radiometric phase correction process entails measuring variations in brightness temperature (T_B^{rms}) with a radiometer, inverting equation (5) to derive the variation in PWV (w_{rms}), and then using equation (6) to derive the variation in electronic phase, ϕ_{rms}, along a given line of sight.

As benchmark numbers for the MMA we set the requirement that we need to measure changes in tropospheric induced phase above a given antenna to an accuracy of $\frac{\lambda}{20}$ at 230 GHz at the zenith, or $\phi_{rms} = 18^o$. This requirement inserted into equation (6) then yeilds a required accuracy of: $w_{rms} = 0.01$ mm. This value of w_{rms} then sets the required sensitivity, T_B^{rms}, of the radiometers as a function of frequency through equation 5. For the VLA we set the $\frac{\lambda}{20}$ requirement at 43 GHz, leading to: $w_{rms} = 0.05$ mm. In its purest form, the inversion of equation (5) requires: (i) a sensitive, absolutely calibrated radiometer, (ii) accurate values for the run of temperature and pressure as a function of height in the atmosphere, and (iii) an accurate value for the height of the PWV fluctuations. We consider the requirements on each of these terms in detail in section 5.

Figure 6 shows the required sensitivity of the radiometer, T_B^{rms}, given the benchmark numbers for w_{rms} for the VLA and the MMA and using equation (5). It is important to keep in mind that lower numbers on this plot imply that more sensitive radiometry is required in order to measure the benchmark value of w_{rms}. Figure 7 shows the detailed behavior of atmospheric brightness temperature, atmospheric transmission, and T_B^{rms} in the vicinity of the water lines at 22.2 GHZ and 183.3 GHz. The required T_B^{rms} values generally increase with increasing frequency due to the increase in A_ν, with a local maximum at the 22 GHz water line, and minima at the strong O_2 lines (59.2 GHz and 118.8 GHz). The strong water line at 183.3 GHz shows a 'double peak' profile, with a local minimum in T_B^{rms} at the frequency corresponding to the peak T_B of the line. This behavior is due to the product: $A_\nu \times e^{-\tau_o}$ in equation 5. The value of A_ν peaks at the line frequency, but this is off-set by the high total optical depth at the line peak. This effect is most dramatic for the VLA case, where the required T_B^{rms} at the 183 GHz line peak is very low.

5. Absolute Radiometric Phase Corrections

5.1. Sensitivity and Gain Stability

In this section we consider making an absolute correction to the electronic phase at a given antenna using an accurate, absolutely calibrated measurement of T_B, and accurate measurements of tropospheric parameters (temperature and pressure as a function of height, and the scale height of the PWV fluctuations). We consider requirements on the gain stability, sensitivity, and on atmospheric data, given the benchmark values of w_{rms} and using equation (5) to relate w_{rms} and T_B^{rms} (see Figures 6 - 9). We consider the requirements at a number of frequencies, including: (i) the water lines at 22.2 GHz and 183.3 GHz, (ii) the half power of the water line at 185.5 GHz, and (iii) two continuum bands at 90 GHz and 230 GHz. For the VLA we only consider the 22.2 GHz line.

The results are summarized in Table 1. Row 1 shows the optical depth per mm PWV,

A_ν, at the different frequencies for the model atmospheres discussed in section 4, while row 2 shows the total optical depth, τ_{tot}, for the models. Row 3 shows the required T_B^{rms} values as derived from equation (5). It is important to keep in mind that these values are simply the expected change in T_B given a change in w of 0.01 mm for the MMA and 0.05 mm for the VLA, for a single radiometer looking at the zenith. All subsequent calculations depend on these basic T_B^{rms} values. The values range from 19 mK at 90 GHz, to 920 mK at 185.5 GHz, at the MMA site, and 120 mK for the VLA site at 22 GHz.

We consider sensitivity and gain stability. Row 4 lists approximate numbers for expected receiver temperatures, $T_{rec+spill}$, in the case of cooled systems (eg. using the astronomical receivers for radiometry). Row 5 lists the contribution to the system temperature from the atmosphere, $T_{rec,atm}$, and row 6 lists the expected total system temperature, T_{tot} (sum of row 4 and 5). Row 7 lists the rms sensitivity of the radiometers, T_{rms}, assuming 1000 MHz bandwidth, one polarization, and a 1 sec integration time. In all cases the expected sensitivities of the radiometers are well below the required T_B^{rms} values, indicating that sensitivity should not be a limiting factor for these systems. Row 8 lists the required gain stability of the system, defined as the ratio of total system temperature to T_B^{rms}: $\delta\mathrm{Gain} \equiv \frac{T_{tot}}{T_B^{rms}}$. Values range from 210 for the 185.5 GHz measurement to 5800 for the 90 GHz measurement at the MMA, and 450 for the VLA site at 22 GHz.

Rows 9 and 10 list total system temperatures and expect rms sensitivities in the case of uncooled radiometers. We adopt a constant total system temperature of T_{tot} = 2000 K, but the other parameters remain the same (bandwidth, etc...). The radiometer sensitivity is then 63 mK in 1 sec. This sensitivity is adequate to reach the benchmark T_B^{rms} values in row 3, although at 230 GHz the sensitivity value is within a factor two of the required T_B^{rms}. The required gain stabilities in this case are listed in row 11. The requirement becomes severe at 230 GHz (δGain = 15000).

5.2. Atmospheric Data

We consider the requirements on atmospheric data, beginning with T_{atm}. The dependence of T_B^{rms} on T_{atm} comes in explicitly in equation (5) through the first multiplier, and implicitly through the effect of T_{atm} on τ_o. For simplicity, we consider only the explicit dependence, which will lead to an underestimate of the expected errors by at most a factor $\approx$ two – adequate for the purposes of this document (Sutton and Hueckstaedt 1997). Under this simplifying assumption the required accuracy, δT_{atm}, becomes:

$$\delta T_{atm} \approx \frac{T_B^{rms}}{[1 - e^{-\tau_o}]} \, K.$$

The values δT_{atm} are listed in row 12. Values in parentheses are the percentage accuracy in terms of the ground atmospheric temperature. Values are typically of order 1 K, or a few tenths of a percent of the mean. A related requirement is the accuracy of the gradient in temperature: $\delta \frac{dT}{dh} \approx \frac{\delta T_{atm}}{h_{turb}}$, in the case of a turbulent layer at $h_{turb} = 2$ km, and assuming a very accurate measurement of T_{atm} on the ground and a very accurate measurement of h_{turb}. These values are listed in row 13 of the table. The accuracy requirements range from 0.25 K km^{-1} to 1.5 K km^{-1}, or roughly 10% of the mean gradient. Similarly, we can consider the required accuracy of the measurement of the height of the troposphere, δh_{turb} $\approx \frac{\delta T_{atm}}{\frac{dT}{dh}}$, assuming a perfect measurement of the ground temperature and temperature gradient. These values are listed in row 14. Values are typically a few tenths of a km, or roughly 10% of h_{turb}.

Finally, we consider the requirements on atmospheric pressure given the T_B^{rms} requirements. The relationship between T_B and w is affected by atmospheric pressure through the change in the pressure broadened line shapes. An increase in pressure will transfer power from the line peak into the line wings, thereby flattening the overall profile. The expected changes in optical depth (or brightness temperature) as a function of frequency have been quantified by Sutton and Hueckstaedt (1997), and their coefficients relating changes in pressure with changes in optical depth are listed in row 17. Note the change in sign of the coefficient on the line peaks versus off-line frequencies. Sutton and Hueckstaedt point out that, since the integrated power in the line is conserved, there are 'hinge-points' in the line profiles where pressure changes have very little effect on T_B, ie. for an increase in pressure at fixed total PWV the wings of the line get broader while peak gets lower. These hinge-points are close to the half power points in T_B of the lines. Rows 15 and 16 list the requirements on the accuracy of P_{atm}, and on the value of h_{turb}. The values of δP_{atm} are derived from the equation: $\delta P_{atm} = \frac{A_\nu w_{rms}}{\tau_{tot} X}$, where X is the coefficient listed in row 17. We find that the value of P_{atm} needs to be known to about 1%, and the height of the turbulent layer needs to be known to a few percent. The exception is at the hinge-point of the line ($\approx$ 185.5 GHz), where the optical depth is independent of P_{atm}.

There are a few potential difficulties with absolute radiometric phase corrections which we have not considered. First, there is the question of how to make a proper measurement of the 'ground temperature'? It is possible, and perhaps likely, that the expected linear temperature gradient of the troposphere displays a significant perturbation close to the ground. The method for making the 'correct' ground temperature measurement remains an important issue to address in the context of absolute radiometric phase correction. Second, we have only considered a simple model in which the PWV fluctuations occur in a narrow layer at some height h_{turb}, which presumably remains constant over time. If the fluctuations are distributed over a large range of altitude then one needs to know the height of the dominant fluctuation at *each time* to convert T_B into electrical pathlength. And when fluctuations at different altitudes contribute at the same time, this conversion becomes problematical. Again, the required accuracies for the height of the fluctuations are given in rows 14 and 16 in Table 1. A possible solution to this problem is to find a linear combination of channels for which the effective conversion factor is insensitive to altitude under a range of conditions (eg. 'hinge points' generalized to a multi-channel approach).

And third, the shape of the pass band of the radiometer needs to be known very accurately in order to obtain absolute T_B measurements.

One final point to keep in mind is that the requirements in Table 1 are all based on the benchmark values for w_{rms} as set by $\frac{\lambda}{20}$ accuracy at 230 GHz for the MMA, and at 43 GHz for the VLA. The values in the table all behave linearly with w_{rms}, and the w_{rms} value behaves linearly with the benchmark frequency. Hence, if we set the more stringent requirement of $\frac{\lambda}{20}$ accuracy at 850 GHz at the MMA, then the requirements in the table become more stringent by the factor: $\frac{230}{850} = 0.27$.

5.3. Model Errors

A final uncertainty involved in making absolute radiometric phase corrections are errors in the theoretical atmospheric models relating w and T_B (section 3). Sutton and Hueckstaedt (1997) point out that model errors are by far the dominant uncertainties when considering absolute radiometric phase correction, and they have calculated a number of models with different line shapes and different empirically determined 'water vapor continuum fudge-factors'. Row 18 in Table 1 lists the approximate differences between the various models at various frequencies. Models can differ by up to 3 mm in PWV, corresponding to 19.5 mm in electrical pathlength, or 30π rad in electronic phase at 230 GHz. The differences are most pronounced in the continuum bands, but are only negligible close to the peak of the strong 183 GHz line. Given the status of current models, radiometric phase correction then requires some form of empirical calibration of the water vapor continuum contribution in order to relate T_B to w. The exception may be a measurement close to the peak of the 183 GHz line, but in this case saturation becomes a problem (section 4). Perhaps most importantly, if the calibrated continuum term is due to incorrect line shapes, it will depend on both T_{atm} and P_{atm}, in which case the continuum term may require frequent calibration.

Overall, absolute radiometric phase correction requires: (i) systems that are sensitive ($19 \leq \mathrm{T}_{rms} \leq 920$ mK), and stable over long timescales ($200 \leq \delta$Gain ≤ 15000), and (ii) knowledge of the tropospheric parameters, such as T_{atm}, P_{atm}, and h_{turb}, to a few percent or less. And even if such accurate measurements are available, fundamental uncertainties in the atmospheric models relating T_B and PWV may require empirical calibration of the T_B^{rms} - w_{rms} relationship at regular intervals.

6. Empirically Calibrated Radiometric Phase Corrections

Many of the uncertainties in Table 1 arise from the fact that we are demanding an absolute phase correction at each antenna based on the measured T_B plus ancillary data (T_{atm}, P_{atm}, h_{turb},...), using a theoretical model of the atmosphere to relate T_B to w. This sets very stringent demands on the absolute calibration, on the accuracy of the ancillary data, and on the accuracy of the theoretical model atmosphere. The current atmospheric models under-predict w by large factors in the continuum bands, thereby requiring calibration of (possibly time dependent) water vapor continuum fudge-factors.

One way to avoid some of these problems is to calibrate the relationship between fluctuations in T_B^{rms} and with fluctuations in antenna-based phase, θ_{rms}, by observing a strong celestial calibrator at regular intervals. This empirically calibrated phase correction method would circumvent dependence on ancillary data and model errors (Woody and Marvel 1998), and mitigate long term gain stability problems in the electronics. This technique can be thought of as calibrating the 'gain' of both the atmosphere and the electronics, in terms of relating T_B^{rms} to θ_{rms} (see section 8).

In its simplest form, empirically calibrated radiometric phase correction would be used only to increase the coherence time on source. No attempt would be made to connect the phase of a celestial calibrator with that of the target source using radiometry, and hence the absolute phase on the target source would still be obtained from the calibration source. Such a process is being implemented at the Owen Valley Radio Observatory (Woody and Marvel 1998). In this case the absolute phase is obtained from the first accurate phase measurement on the celestial calibrator, while the subsequent time series of phase measurements on the calibrator are then used to derive the T_B^{rms} to θ_{rms} relationship. This process results in additional phase uncertainty in a manner analagous to Fast Switching phase calibration (Holdaway and Owen 1995). The residual error is set by the distance between the calibrator and source, and the time required to obtain the first accurate record: $t_{cal} \equiv$ (the slew time + the integration time required for the first accurate phase measurement). In this case:

$$b_{eff} \;\approx\; V_A \times t_{cal} \;+\; d,$$

where d is the physical distance in the troposphere set by the angular separation of the calibrator and the source, and b_{eff} is the 'effective baseline' to be inserted into equation 2 in order to estimate the residual uncertainty in the absolute phase. For example, assuming t_{cal} = 10 sec, and the calibrator-source separation = 2^o, leads to b_{eff} = 170 m, or ϕ_{rms} = 22^o at 230 GHz. Note that the temporal character of this 'phase noise' is unusual in that the short timescale ($t << t_{cyc}$) variations are removed by radiometry, while the long timescale variations ($t >> t_{cyc}$) are removed by celestial source calibration.

It may be possible to use empirically calibrated radiometric phase corrections to both increase the coherence time on source, and to connect the phase between the celestial calibrator and the target source. Whether this technique is viable depends on a number of factors, including: (i) the distance between the source and calibrator, (ii) the flux density of the calibrator, and (iii) the time scale for changes in the 'atmospheric gain', ie. changes in the T_B^{rms} - θ_{rms} relationship.

7. Other Issues

7.1. Clouds

Water droplets present the problem that the drops contribute significantly to the measured T_B but not to w, thereby invalidating the model relating T_B and w. This problem can be avoided by using multichannel measurements around the water lines (183 GHz or 22 GHz), since T_B for the lines is not affected by water drops. Alternatively, a dual-band system could be used to separate the effect of water drops from water vapor (eg. 90 GHz and 230 GHz), since the frequency dependence of T_B is different for the two water phases. This later method requires a multi-band radiometer, which may be difficult within the context of the MMA antenna design. The question of whether clouds will be a significant problem on the Chajnantor site remains to be answered.

7.2. Electronic Phase

We have ignored the electronic phase term, which can have a long term component and possibly a short term ('noise') component. The long term component can be calibrated using observations of a celestial calibrator at the target source frequency at regular intervals. The electronic noise term can be reduced through careful design of the electronics, although the degree to which this noise can be reduced remains uncertain. At the VLA the electronic noise increases as roughly 0.5^o per GHz. The electronic noise term will add to the tropospheric noise term in all the techniques described above, with the exception of Fast Switching in the case where both target source and calibrator are observed at the same frequency.

8. Intermediate Solutions: An Alternate Approach

In this section we present an alternate formulation of the radiometric phase correction technique, illustrating the relaxed requirements on the atmospheric model when the elements of an interferometer observe through a common atmosphere.

There are at least three different scenarios for radiometric correction, each with different calibration demands. They are: 1) observing with a single antenna through one column of atmosphere; 2) observing with two or more antennas that share an atmosphere with common properties; 3) as for previous case, but including phase referencing to a calibrator source.

8.1. Single column

Consider the case of a radiometer used to measure the fluctuations in the electrical path length through a column of the Earth's atmosphere. If it has one frequency channel, then the output is brightness temperature $T_{\rm rad}$ which is related to the true brightness temperature T through a gain factor: $T_{\rm rad} = GT$. We write $G = 1 + \delta G$; the error term δG accounts for the passband of the channel not being known precisely and temporal variations in the instrument response that are not calibrated out. The extra electrical path length L through this atmospheric column is calculated using a conversion factor M derived from a model of the atmosphere: $L = MGT$. In general, M is not equal to the optimum value M_o, and $M = M_o + \delta M$. The radiometer may have multiple channels, in which case a linear combination of the measured brightness temperatures $\Sigma W_{\rm i} G_{\rm i} T_{\rm i}$ replaces GT.

The fluctuations in the column of water vapor typically represent only a small fraction (5 to 10%) of the total water vapor column. We write $L = \overline{L} + \delta L$ and $T = \overline{T} + \delta T$. The average path excess is estimated by $\overline{L} = 6.5w/\sin\epsilon$, where w is the precipitable water vapor and ϵ is the elevation above the horizon. Measuring L to within 30 μm under typical conditions ($w = 1$ mm, $\epsilon = 45°$) requires $\delta M/M$ and $\delta G/G$ to be less than 0.3%. For $w = 3$ mm and $\epsilon = 20°$ the requirement becomes 0.05%. The gain stability is a lower limit, since the noise temperature of the radiometer itself has been neglected.

This is the 'absolute' correction scheme examined earlier. It is relevant for cases with a single, isolated line of sight, such as telemetry to a satellite or planetary probe, or a VLBI experiment where each antenna is observing under different conditions.

8.2. Differential column

Phase correction for a connected-element interferometer requires a measurement of the difference in L between two parallel columns through the atmosphere:

$$
\begin{aligned}
L_1 - L_2 &= M_1 G_1 T_1 - M_2 G_2 T_2 && (1) \\
&\simeq M_o(\delta T_1 - \delta T_2) + M_o \overline{T}(\delta G_1 - \delta G_2) && (2)
\end{aligned}
$$

The approximation is correct to first order in small quantities. The first term is the desired quantity and the second represents the error. It has been assumed that the structure of the atmosphere is similar enough for the two lines of sight that $\delta M_1 = \delta M_2$. This may not be true for very long baselines. It is also assumed that $\overline{T}_1 = \overline{T}_2$; this will not be the case if there is a difference in altitude between the radiometers.

Measuring $L_1 - L_2$ to within 30 μm requires $(\delta G_1/G_1 - \delta G_2/G_2)$ to be less than 0.3% for $w = 1$ mm and $\epsilon = 45°$, or less than 0.05% for $w = 3$ mm and $\epsilon = 20°$. In this case a constant offset is generally not important, and the challenge is stabilizing or calibrating out the time-varying part of the radiometer gains. Note that there is very little dependence on the model; this is because $\overline{L}$, which represents almost all of the excess path along each column, is common to all antennas and cancels out.

8.3. Differential column with phase referencing

Calibration of an interferometer's instrumental response requires regular measurements of a calibrator source. At a given time, there will in general be a different $L_1 - L_2$ for atmospheric paths to the calibrator compared to the value for the target. This change needs to be measured by the radiometers to avoid the associated phase error, which can be substantial (Lay 1997).

If the target is at elevation $\epsilon 1$ and the calibrator at elevation $\epsilon 2$ then to first order in the uncertainties

$$\begin{aligned}\{L_1 - L_2\}_{\epsilon 1} - \{L_1 - L_2\}_{\epsilon 2} \;\simeq\;& \{\delta L_1 - \delta L_2\}_{\epsilon 1} - \{\delta L_1 - \delta L_2\}_{\epsilon 2} + \\ & (M_{o,\epsilon 1}\overline{T}_{\epsilon 1} - M_{o,\epsilon 2}\overline{T}_{\epsilon 2})(\delta G_1 - \delta G_2). \qquad (3)\end{aligned}$$

The first two terms represent the actual change in differential path length and the third is the primary source of error. For typical conditions ($\epsilon 1 = 44°$, $\epsilon 2 = 46°$, $w = 1$ mm), the first factor gives 0.32 mm, so that $(\delta G_1 - \delta G_2)$ must be less than 0.1 for 30 μm accuracy. For a more extreme water column and elevation change ($\epsilon 1 = 18°$, $\epsilon 2 = 22°$, $w = 3$ mm), the first factor gives 11 mm, so that $(\delta G_1 - \delta G_2)$ must be less than 0.003 for 30 μm accuracy. This is a requirement on the agreement between the two radiometers, rather than on time stability of the gains, i.e. if the radiometers were looking at the same column of water, they must give the same value of L to within 0.3% to satisfy the worst case scenario. Again, note that there is little dependence on the model.

8.4. Models and empirical data

The required accuracy of the conversion factor M is set by the dynamic range needed in measuring the fluctuations. If the rms path length fluctuation is 300 μm and the residual rms needed is less than 30 μm, then M must be known to better than 10% (a much less stringent requirement than for the single column absolute case). The value of M can be determined either from an atmospheric model or empirically by comparing the actual path length fluctuations measured by the interferometer on a bright source to those derived from the radiometers. The two can be used together, so that the atmospheric model is continually refined by the measured values.

9. Conclusions

We have considered various limitations on radiometric phase correction techniques in the context of the MMA at Chajnantor, and for the VLA. The benchmark requirements are set as $\frac{\lambda}{20}$ at 230 GHz for the MMA, and at 43 GHz for the VLA. Sensitivity of the radiometers does not appear to be a limiting factor. In all cases the expected radiometer sensitivity is at least a factor of a few below the required values. Required sensitivities range from 20 mK at 90 GHz to 1 K at 185 GHz for the MMA, and 120 mK for the VLA at 22 GHz. Gain stability requirements may prove to be a limitation, in particular for uncooled radiometers. The minimum requirement is about 200 at 185 GHz at the MMA assuming that the astronomical receivers are used for radiometry. This increases to 2000 for an uncooled system. The stability requirement is 450 for the cooled system at the VLA at 22 GHz. Note that if we set the more stringent requirement of $\frac{\lambda}{20}$ accuracy at 850 GHz at the MMA, then the requirements in the table become more stringent by the factor: $\frac{230}{850}$ = 0.27.

We consider making an absolute correction to the electronic phase at a given antenna using an accurate, absolutely calibrated measurement of T_B, and accurate measurements of tropospheric parameters. Converting the measured T_B to electrical pathlength requires knowledge of the tropospheric parameters, such as T_{atm}, P_{atm}, and h_{turb}, to a few percent or less. And even if such accurate measurements are available, fundamental uncertainties in the atmospheric models relating T_B and PWV may require empirical calibration of the T_B^{rms} - w_{rms} relationship at regular intervals.

We then consider the less demanding technique of making radiometric phase corrections using an empirical calibration of the T_B^{rms} - θ_{rms} relationship to increase the coherence time on source, and perhaps to connect the target source phase to a celestial calibrator. A number questions remain to be answered concerning this technique, including: (i) over what time scale and distance will this technique allow for radiometric phase corrections when switching between the the source and the calibrator?, and (ii) how often will calibration of the T_B^{rms} - θ_{rms} relationship be required, ie. how stable are the mean parameters of the atmosphere (eg. pressure, temperature, height of the turbulence)? These questions can only be answered through extensive testing at a particular site. If empirically calibrated radiometry cannot be used to transfer the phase between the source and calibrator, the residual uncertainty in the absolute phase on the target source will depend on the distance between the source and calibrator, and on the time required for the first accurate phase measurement on the calibrator, in a manner analogous to errors induced when using Fast Switching phase calibration.

Overall, we feel that multifrequency measurements around the water lines (22 GHz and 183 GHz) appear to be the most promising technique, since the hinge points of the line ($\approx$ half-power) are insensitive to atmospheric parameters, and clouds are automatically excluded. For the MMA multifrequency measurements around the 183 GHz line have the additional advantages that the model uncertainties are minimized, as are the requirements on gain stability. Also, it may be possible to use the astronomical receiver system to make these measurements, depending on the final system design. One possible problem is saturation of the line in poor weather. We are currently performing simulations to test how sensitive the PWV measurements are for different line strengths using various combinations of frequencies across the 183 GHz line.

Table 1. Limits to Absolute Radiometric Phase Calibration

		22.2 GHz	90	183.3	185.5	230	22.2 (VLA)
1	A_ν mm^{-1}	0.0115	0.0073	2.79	0.670	0.053	0.0085
2	τ_{tot}	0.0167	0.028	2.79	0.677	0.057	0.043
3	T_B^{rms} mK	30	19	460	920	135	120
4	$T_{rec+spill}$ K	40	100	100	100	100	40
5	$T_{rec,atm}$ K	7	10	246	94	20	14
6	T_{tot} K	47	110	346	194	120	54
7	T_{rms} mK	1.4	3.5	11	6	3.8	1.7
8	δGain	1600	5800	750	210	890	450
9	T_{tot} K	–	–	2000	2000	2000	–
10	T_{rms} mK	–	–	63	63	63	–
11	δGain	–	–	4400	2200	15000	–
12	δT_{atm} K	1.8 (0.7%)	0.7 (0.3%)	0.5 (0.2%)	1.9 (0.7%)	2.4 (0.9%)	2.9 (1.0%)
13	$\delta \frac{dT_{atm}}{dh}$ K/km	0.9 (14%)	0.35 (5%)	0.25 (4%)	1.0 (15%)	1.2 (18%)	1.5 (22%)
14	δh_{turb} km	0.28 (14%)	0.11 (5%)	0.08 (4%)	0.29 (15%)	0.37	0.45 (22%)
15	δ P_{atm} mb	-5 (0.9%)	2 (0.3%)	-7.5 (1.3%)	inf	7 (1.2%)	-7.4 (1.0%)
16	δh_{turb} km	0.07 (3%)	0.03 (1.5%)	0.1 (5%)	inf	0.1 (5%)	0.1 (5%)
17	$\frac{1}{\tau_{tot}} \frac{d\tau}{dP}$ mb^{-1}	-0.00133	0.00133	-0.00133	0	0.00133	-0.00133
18	δ(Model w) mm	0.2	3	0.0025	0.01	3	4.8

Description of quantities in Table 1

Basic Assumptions: $\phi_{rms} = 18^o$ ($\frac{\lambda}{20}$) at 230 GHz (MMA) and 43 GHz (VLA), and w_o = 1mm (MMA) and 4mm (VLA)

$\mathbf{A}_\nu$: Optical depth per mm of water.

τ_{tot}: Total optical depth of the model (H_2O plus O_2 plus trace gases).

$\mathbf{T}_B^{rms}$: Required rms of the measured brightness temperature to meet the $\frac{\lambda}{20}$ standards given above.

$\mathbf{T}_{rec+spill}$: Total system temperature excluding the atmospheric contribution.

$\mathbf{T}_{rec,atm}$: Atmospheric contribution to the system temperature.

$\mathbf{T}_{tot}$: Total system temperature on sky. Note: two different assumptions are made at a few frequencies, for cooled and uncooled systems (see section 5.1). Row 6 gives the case of a cooled receiver (eg. using the astronomical receivers for radiometry). Row 9 gives the case of an uncooled receiver.

$\mathbf{T}_{rms}$: Expected rms noise in 1 sec with 1 GHz bandwidth and 1 polarization.

δ**Gain:** Required gain stability in order to obtain T_B^{rms}.

$\delta\mathbf{T}_{atm}$: Required accuracy of the measurement of the atmospheric temperature (in the turbulent layer) in order to obtain T_B^{rms}. Values in parentheses indicate the percentage of the total.

$\delta\frac{dT_{atm}}{dh}$: Required accuracy of the measurement of the gradient in atmospheric temperature, assuming T_{atm} is measured very accurately on the ground and extrapolated to h_{turb}.

$\delta\mathbf{h}_{turb}$**:** Required accuracy of the measurement of the height of the turbulent layer given the δT_{atm} requirement.

$\delta\mathbf{P}_{atm}$**:** Required accuracy of the measurement of the atmospheric pressure (in the turbulent layer) in order to obtain T_B^{rms}.

$\delta\mathbf{h}_{turb}$**:** Required accuracy of the measurement of the height of the turbulent layer given the δP_{atm} requirement.

$\frac{1}{\tau}\ \frac{d\tau}{dP}$**:** Constants used to relate changes in pressure to changes in optical depth as a function of frequency (Sutton and Hueckstaedt 1997).

δ**(Model w):** Differences between various model atmospheres involving different line shapes and different 'water vapor continuum fudge-factors' relating the measured T_B to w (Sutton and Hueckstaedt 1997).

References

Bagri, D.S. 1994, VLA Test Memo. No. 184

Barrett, A.H. and Chung, V.K. 19962, J. Geophys. Res., 67, 4259

Bremer, M., Guilloteau, S., and Lucas, R., in *Science with Large Millimetre Arrays*, eds. P. Shaver (ESO: Garching)

Carilli, C.L., Holdaway, M.A., and Sowinski, K. 1996, VLA Scientific Memo. No. 169

Carilli, C.L. and Holdaway, M.A. 1996, VLA Scientific Memo. No. 171

Carilli, C.L. and Holdaway, M.A. 1996, MMA Scientific Memo. No. 173

Dicke, R.H., Beringer, R., Kyhl, R.L., and Vane, A.B. 1946, Physical Review, 70, 340

Coulman, C.E. 1990, in *Radio Astronomical Seeing*, eds. J. Baldwin and S. Wang, (Pergamon: New York), p. 11.

Garratt, J.R. 1992, *The Atmospheric Boundary Layer*, (Cambridge Univ. Press: Cambridge), p. 11.

Hinder, R. and Ryle, M. 1971, M.N.R.A.S., 154, 229

Hogg, D.C., Guiraud, F.O., and Decker, M.T. 1981, A&A, 95, 304

Holdaway, M.A., Radford, S., Owen, F., and Foster, S. 1995, MMA Memo. Series.

Holdaway, M.A. and Owen, F.N. 1995, MMA Memo. No. 126

Holdaway, M.A. Owen, F., and Rupen, M.P. 1994, MMA Memo. No. 123

Holdaway, M.A. 1992, MMA Memo. No. 84

Holdaway, M.A. and Pardo, J.R. 1997, MMA Memo. No. 187

Liebe, H.J. 1989, International Journal of Infrared and Millimeter Waves, 10, 631

Lay, O.P. 1997, A&A (supp), 122, 547

Lay, O.P. 1997, A&A (supp), 122,535

Resch, G.M., Hogg, D.E., and Napier, P.J. 1984, Radio Science, 19, 411

Rosenkranz, P. 1989, in *Atmospheric Remote Sensing by Microwave Radiometry*, ed. M. Janssen, (New York: Wiley and Sons)

Sramek, R. 1990, in *Radio Astronomical Seeing*, eds. J. Baldwin and S. Wang, (Pergamon: New York), p. 21

Staelin, D.H. 1966, J. Geophys. Res., 71, 2875

Sutton, E.C. and Hueckstaedt, R.M. 1997, A&A (supp), 119, 559

Tatarskii, V.I. 1961, Wave Propagation in Turbulent Media, (New York: Wiley)

Taylor, G.I. 1938, Proc. R. Soc. London A, 164, 476

Welch, W.J. 1994, in *Astronomy with Millimeter and Submillimeter Wave Interferometry*, eds. M. Ishiguro and W.J. Welch, (San Francisco: PASP), p. 1

Westwater, E.R. and Guiraud, F.O. 1980, Radio Science, 15, 947

Woody, D. and Marvel, K. 1998, www.ovro.caltech.edu

Wright, M.C.H. 1996, P.A.S.P., 108, 520

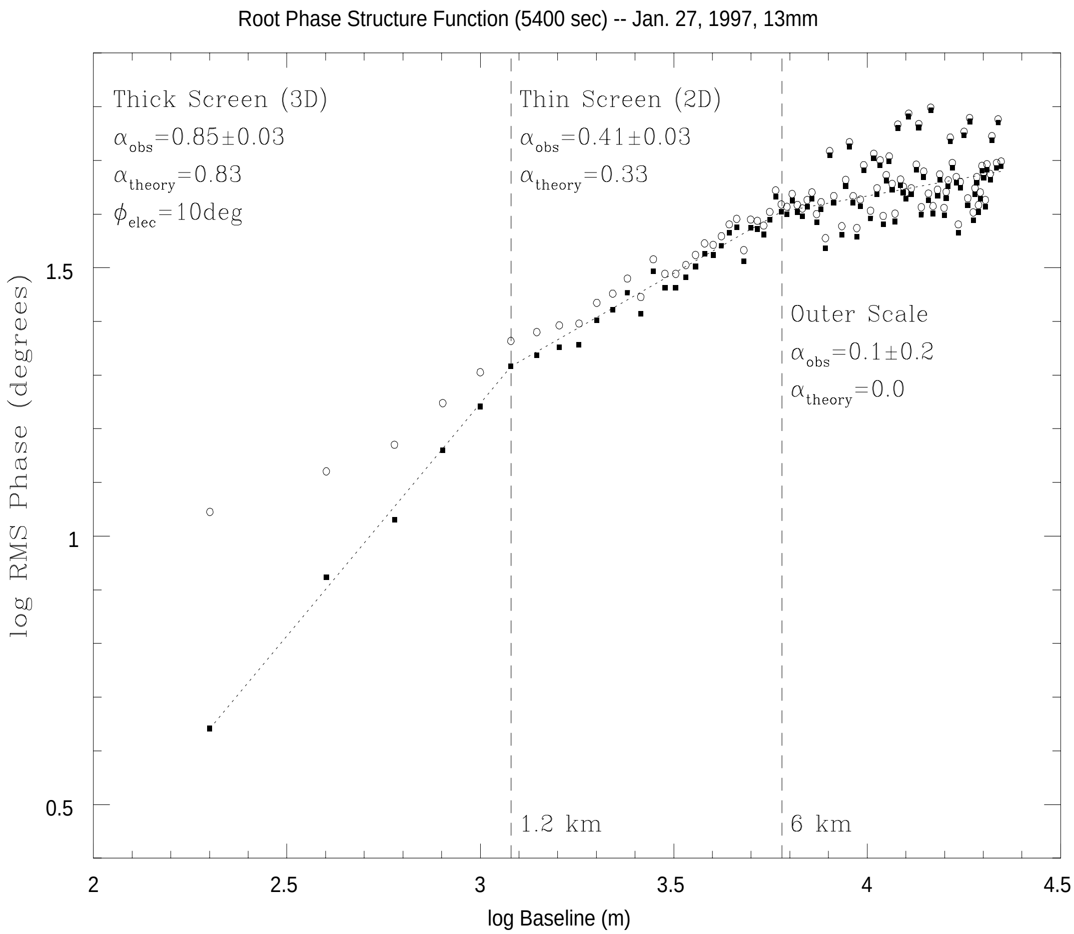

Fig. 1.— The root phase structure function from observations at 13 mm in the BnA array of the VLA on January 27, 1997 (from Carilli and Holdaway 1997). The open circles show the rms phase variations versus baseline length measured on the VLA calibrator 0748+240 over a period of 90 min. The filled squares show these same values with a constant noise term of 10° subtracted in quadrature. The three regimes of the root phase structure function as predicted by Kolmogorov turbulence theory are indicated.

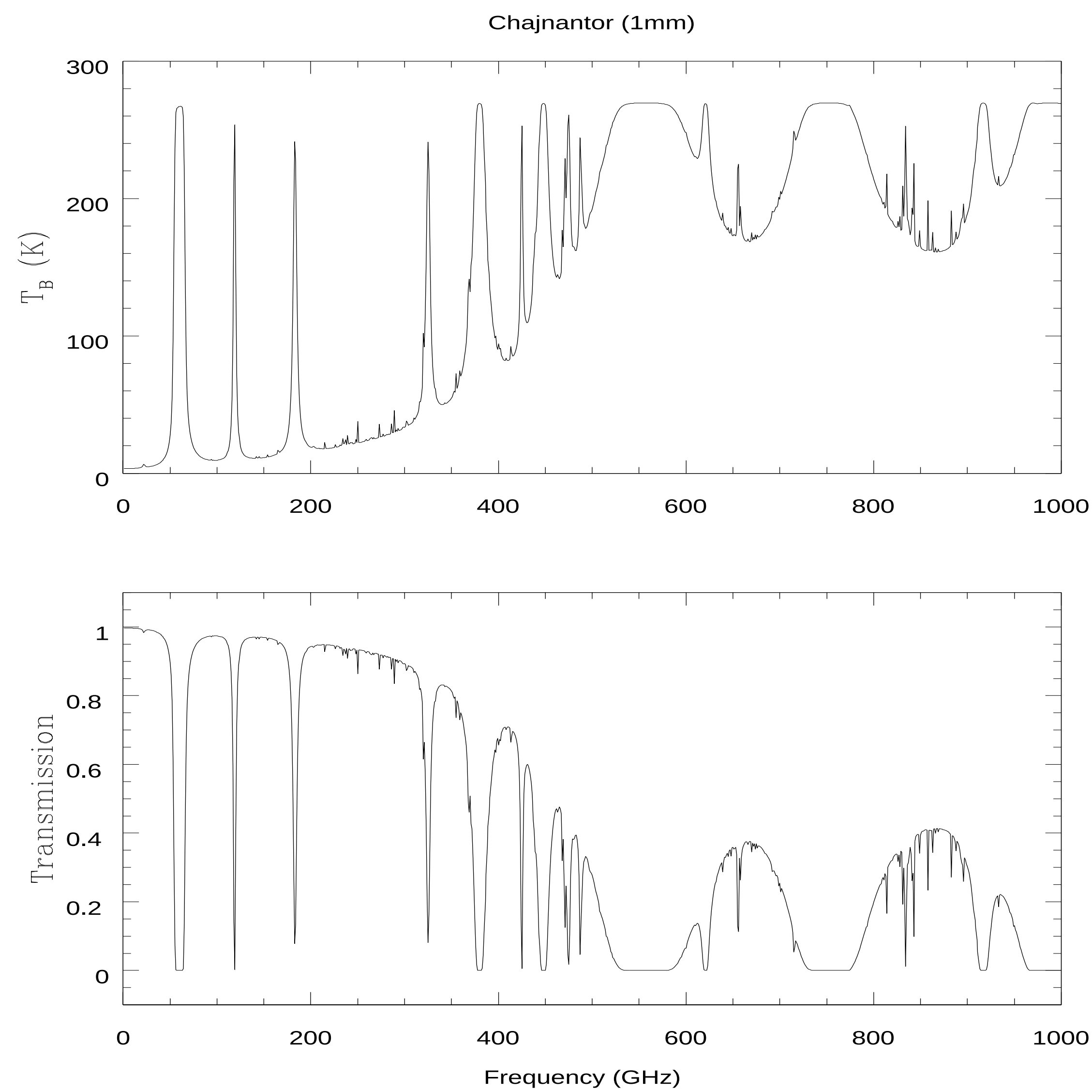

Fig. 2.— The upper frame shows the radiometric brightness temperature of the atmosphere for the MMA site at Chajnantor assuming 1 mm of PWV using the Liebe model (1989). The lower frame shows the corresponding transmission.

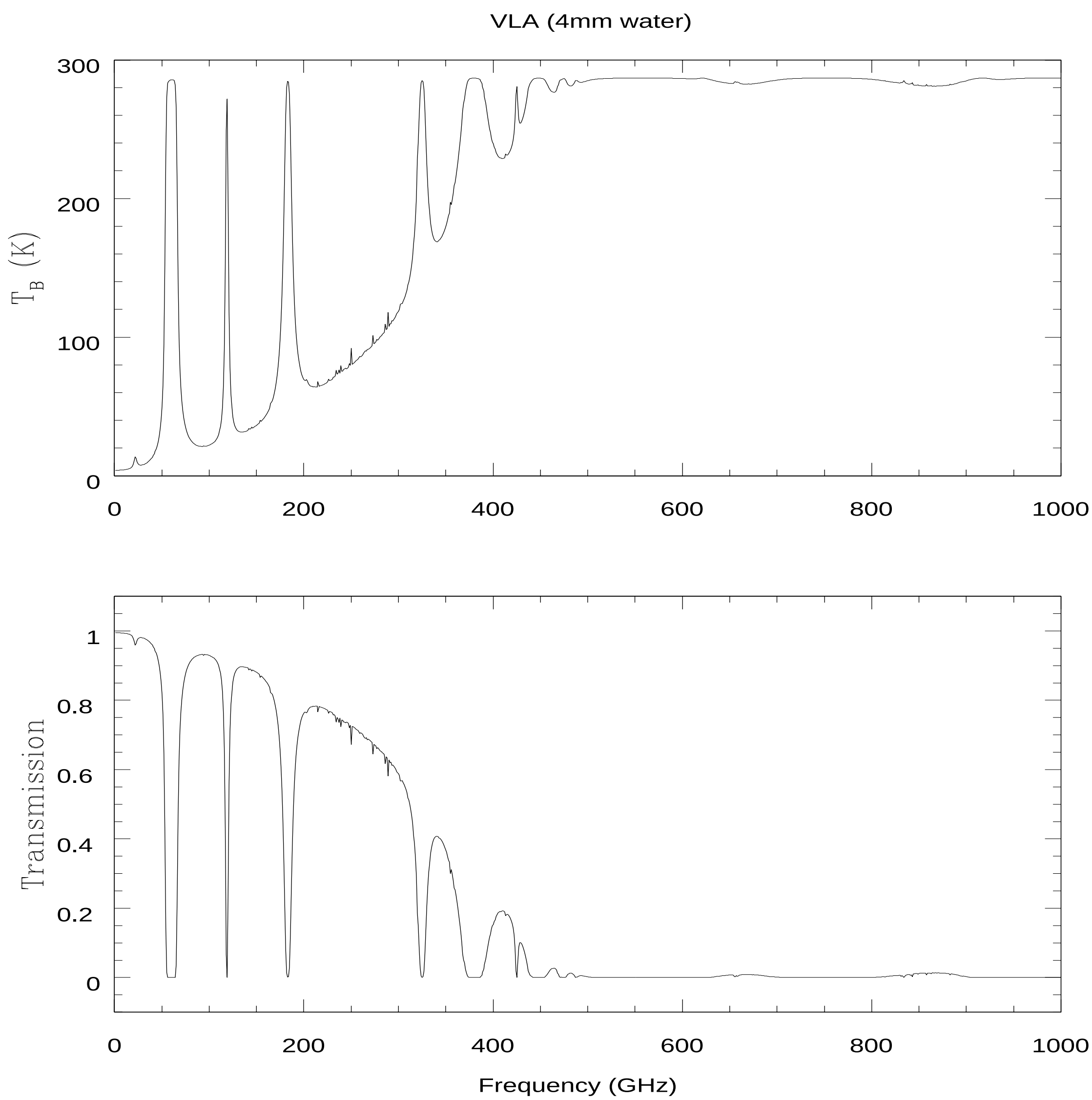

Fig. 3.— The upper frame shows the radiometric brightness temperature of the atmosphere for the VLA site assuming 4 mm of PWV. The lower frame shows the corresponding transmission.

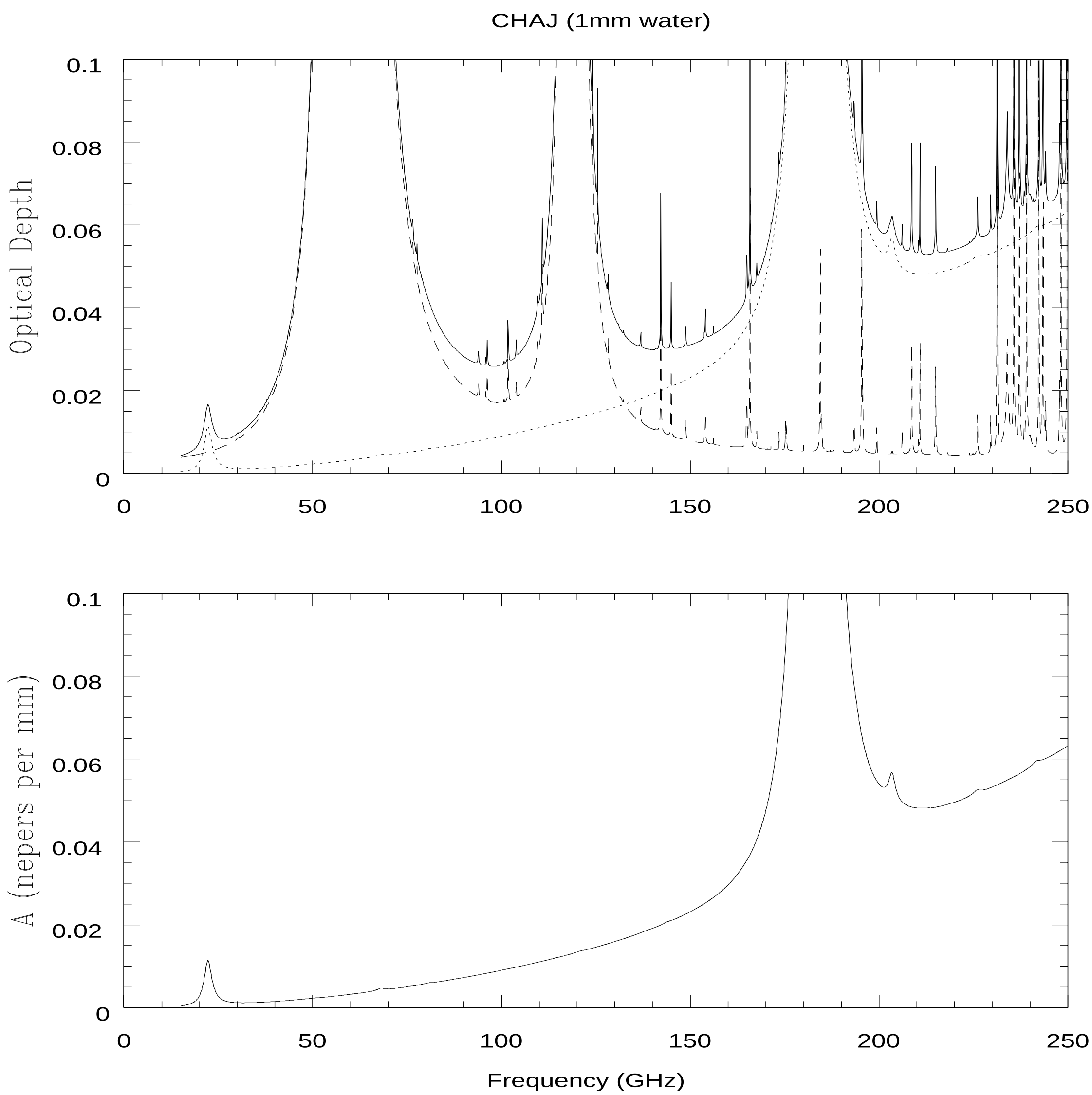

Fig. 4.— The upper frame shows the optical depth for MMA site at Chajnantor assuming 1 mm of PWV. The solid line is the total optical depth. The dotted line is the optical depth due to PWV. The dash line is the optical depth due to O_2 and other trace gases. The lower frame shows A_ν = optical depth due to 1 mm pf PWV.

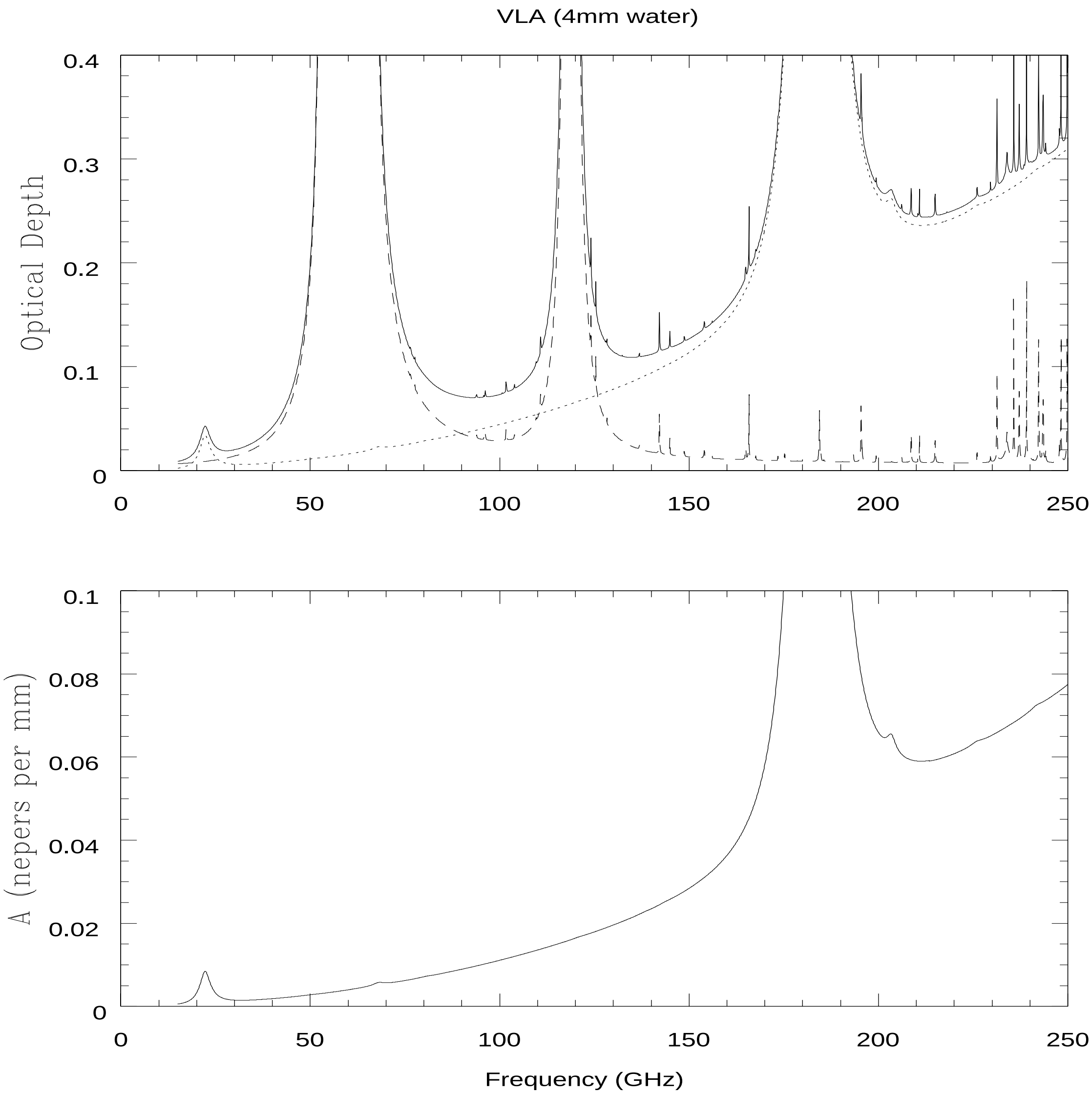

Fig. 5.— The upper frame shows the optical depth for VLA site assuming 4 mm of PWV. The solid line is the total optical depth. The dotted line is the optical depth due to PWV. The dash line is the optical depth due to O_2 and other trace gases. The lower frame shows A_ν = optical depth due to 1 mm pf PWV.

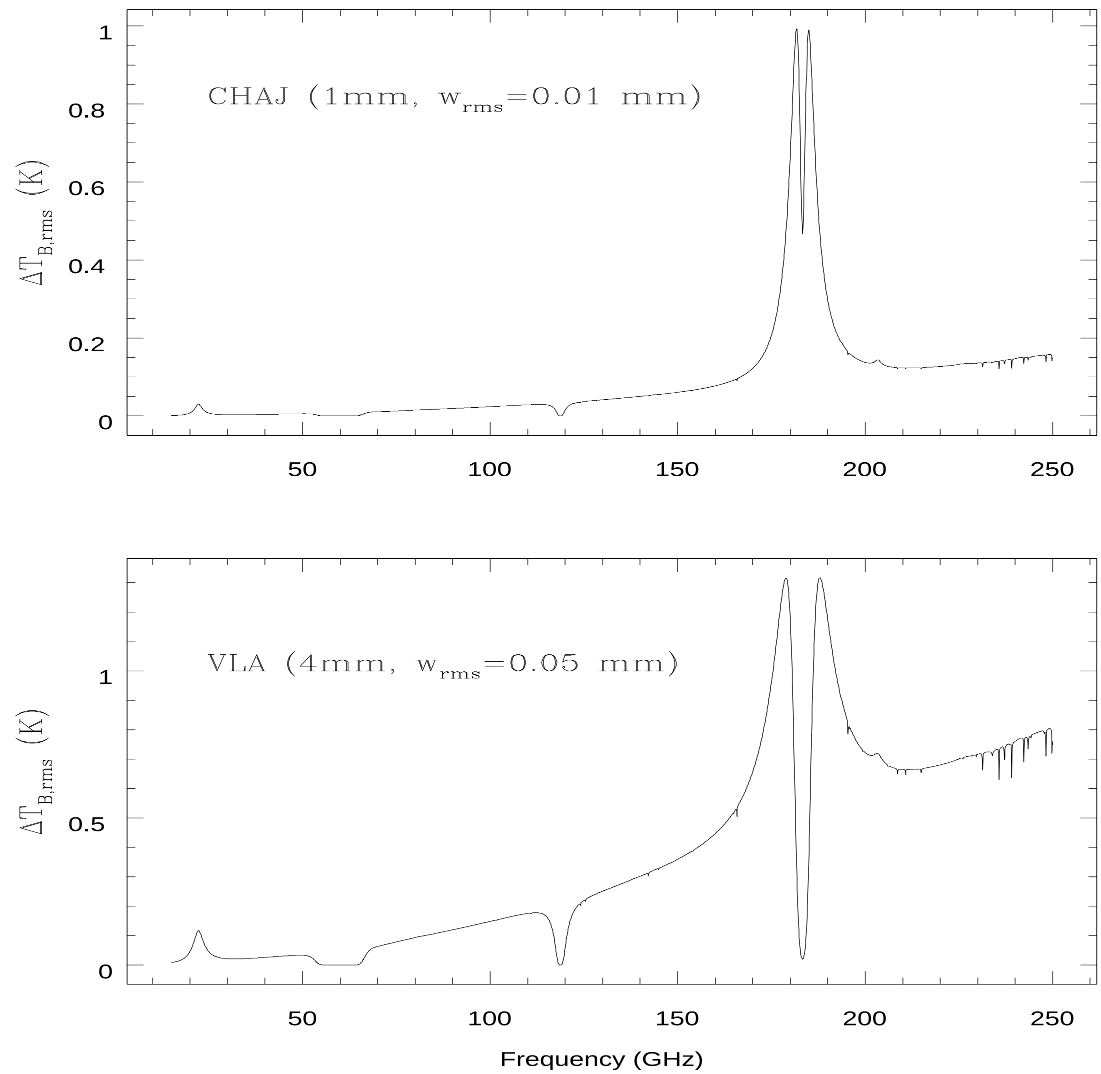

Fig. 6.— The upper frame shows the expected T_B^{rms} for the MMA site at Chajnantor assuming 1 mm of PWV, and w_{rms} = 0.01 mm (equation 5). The bottom frame shows the expected T_B^{rms} for the VLA site assuming 4 mm of PWV, and w_{rms} = 0.05 mm.

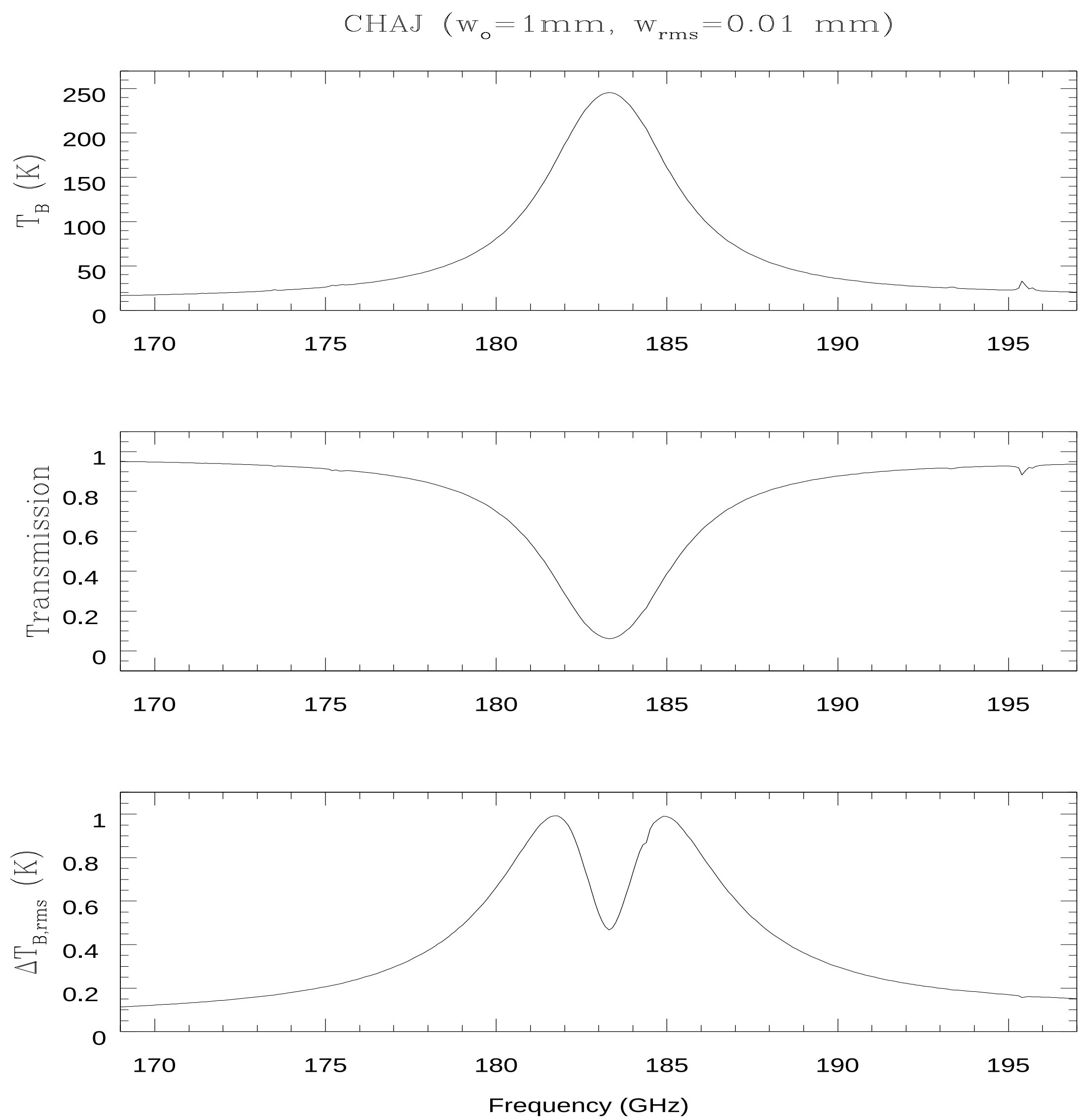

Fig. 7.— The upper frame shows the expected T_B for 183 GHz line for the MMA site at Chajnantor assuming 1 mm of PWV. The middle frame shows the transmission in this frequency range. The bottom frame shows the expected T_B^{rms} assuming $w_{rms} = 0.01$ mm.

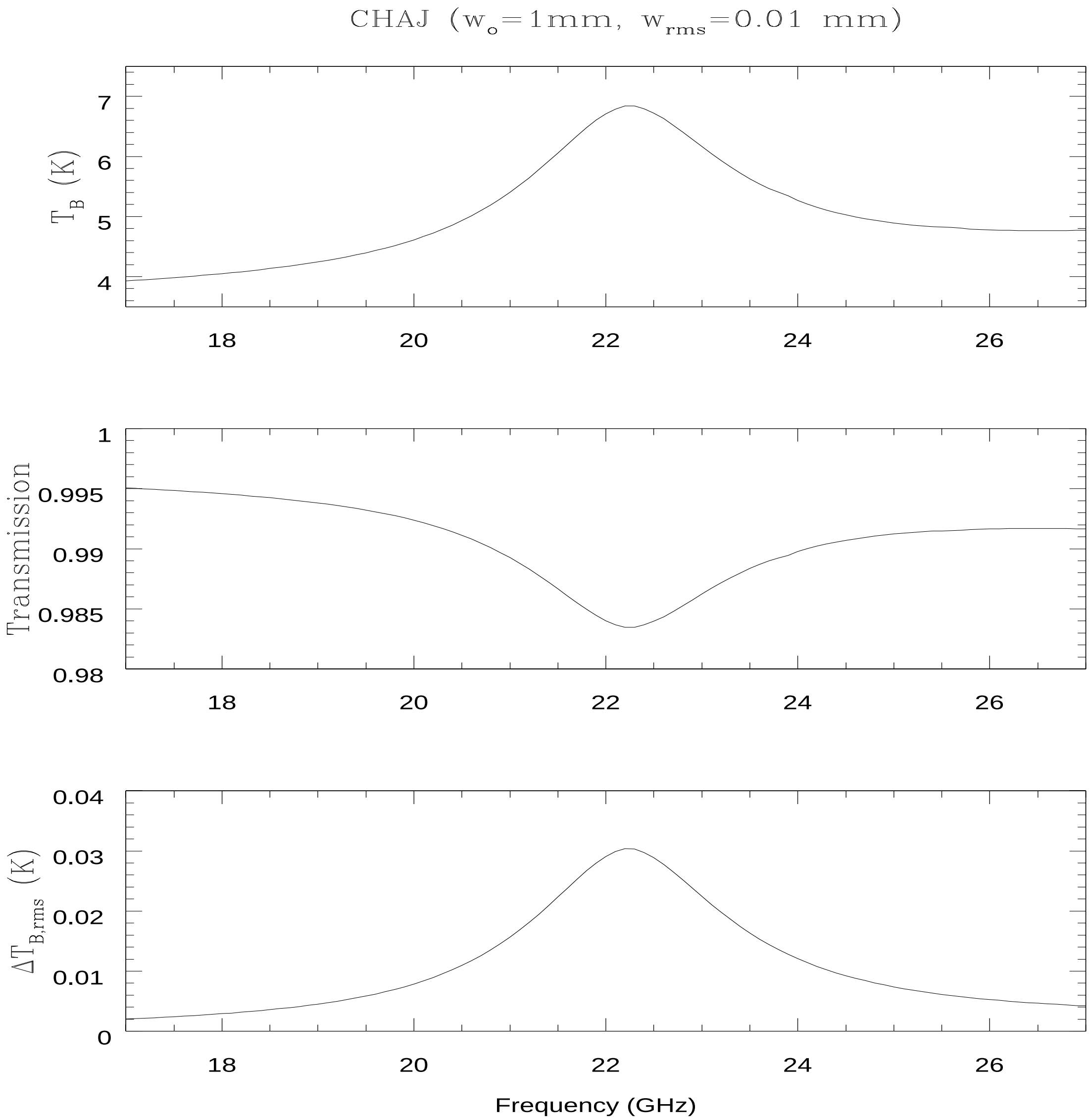

Fig. 8.— The upper frame shows the expected T_B for 22 GHz line for the MMA site at Chajnantor assuming 1 mm of PWV. The middle frame shows the transmission in this frequency range. The bottom frame shows the expected T_B^{rms} assuming w_{rms} = 0.01 mm.

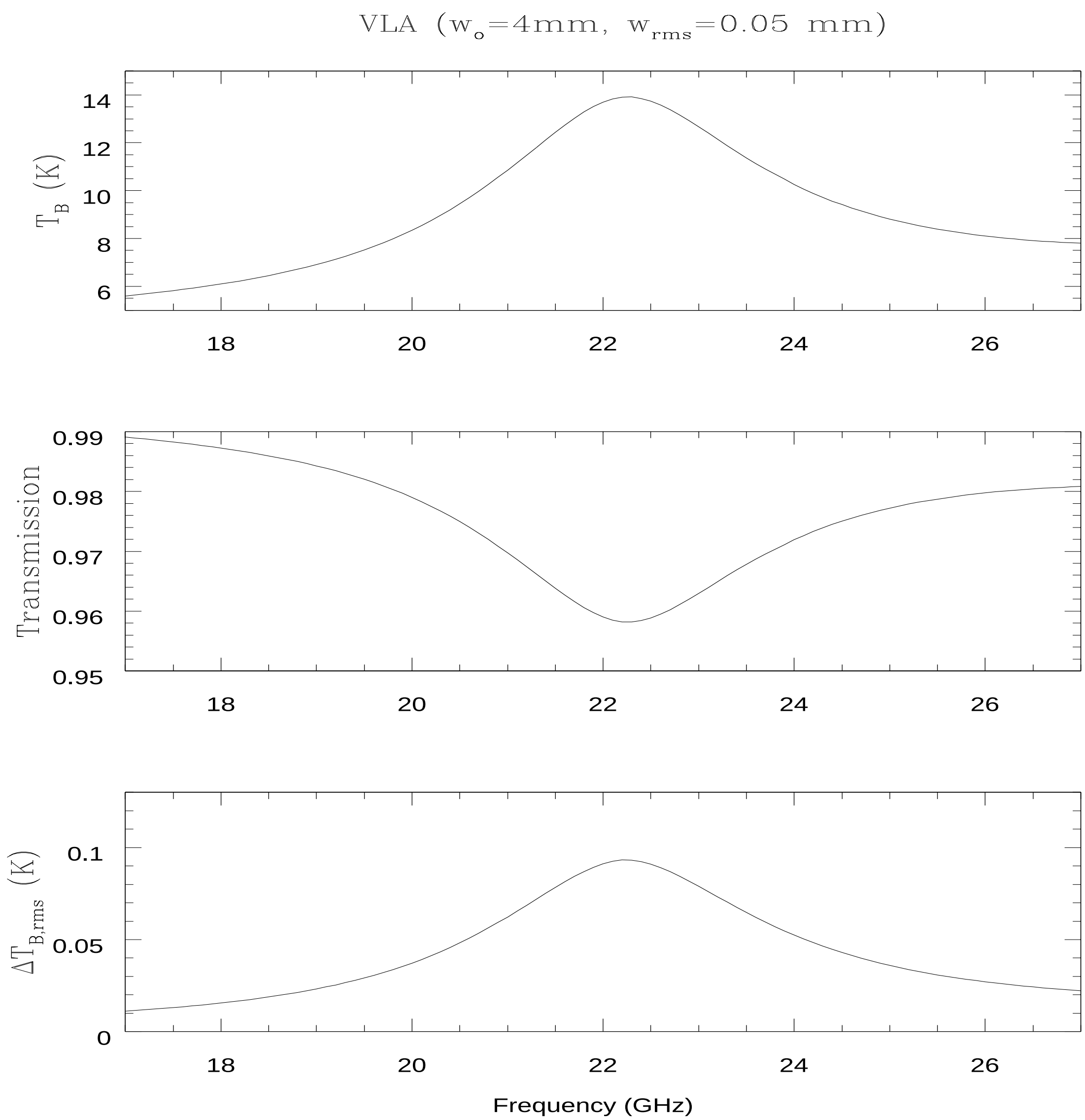

Fig. 9.— The upper frame shows the expected T_B for 22 GHz line for the VLA site assuming 4 mm of PWV. The middle frame shows the transmission in this frequency range. The bottom frame shows the expected T_B^{rms} assuming $w_{rms} = 0.05$ mm.